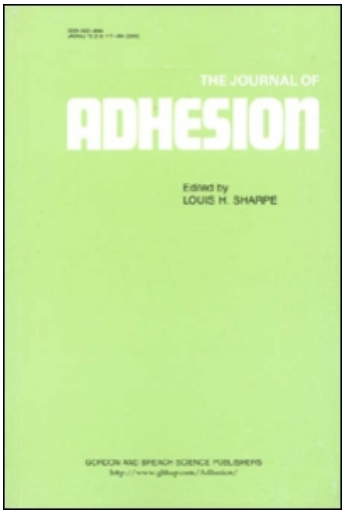

The Journal of Adhesion
Publication details, including instructions for authors and subscription information:
http://www.informaworld.com/smpp/title~content=t713453635

Peeling of Acrylic Pressure Sensitive Adhesives: Cross-Linked versus Uncross-Linked Adhesives

C. Verdier[ab]; J. -M. Piau[ab]; L. Benyahia[ab]
[a] Laboratoire de Rhéologie, Domaine Universitaire, Grenoble, Cedex, France [b] Université Joseph Fourier Grenoble 1, Institut National Polytechnique de Grenoble,

To cite this Article Verdier, C. , Piau, J. -M. and Benyahia, L.(1998) 'Peeling of Acrylic Pressure Sensitive Adhesives: Cross-Linked versus Uncross-Linked Adhesives', The Journal of Adhesion, 68: 1, 93 — 116
To link to this Article: DOI: 10.1080/00218469808029581
URL: http://dx.doi.org/10.1080/00218469808029581

J. Adhesion, 1998, Vol. 68, pp. 93 - 116
Reprints available directly from the publisher
Photocopying permitted by license only

Peeling of Acrylic Pressure Sensitive Adhesives: Cross-Linked versus Uncross-Linked Adhesives

C. VERDIER**, J.-M. PIAU and L. BENYAHIA

Laboratoire de Rhéologie, Domaine Universitaire, BP 53, 38041 Grenoble Cedex 9, France*

(Received 13 October 1997; In final form 15 December 1997)

In this paper we analyze the adhesive properties of two kinds of adhesives, determined by a 90° peeling test on a Pyrex™ substrate. Simultaneously, we observe the mechanisms of flow at the peeling front. An uncross-linked acrylic pressure-sensitive adhesive is used, whereas the second one, of the same class, is slightly cross-linked. The mechanisms of peeling are compared with the ones of our previous study (Benyahia *et al.* [8]) and are found to be identical in the case of uncross-linked adhesives. On the other hand, we find new regimes of flow when the adhesive is cross-linked.

To investigate these differences further, we determine the rheometrical properties of the adhesives in dynamic shear tests and in uniaxial elongational experiments. Furthermore, surfaces are characterized.

A discussion of the peeling curves is finally presented, showing the combined effects of the rheological properties and the surface ones. Conditions for predicting the type of regimes and transitions are also investigated.

Keywords: Adhesion; rheology; acrylic; pressure-sensitive adhesive; peel; surface energy; mechanisms; cross-linking

1. INTRODUCTION

The importance of the rheological properties in the study of adhesives is not new [1], and it is a real challenge to be able to predict the

* Université Joseph Fourier Grenoble 1, Institut National Polytechnique de Grenoble, CNRS (UMR 5520).
**Corresponding author.

adhesive resistance of a given bond in terms of surface energies and the rheometrical properties of the adhesive. To be able to predict the peel resistance of an adhesive, one can think of observing closely the mechanisms of peeling occurring at the peeling front. Kaelble [2] was the first one to look at the peeling front with a special device allowing him to come up with a stress distribution as the adhesive moves toward the detachment point. Later, Niesolowski *et al.* [3] took photographs of the front and measured the backing curvature to determine the force required in a peel test. Zosel [4] looked at some mechanisms occurring in a tack test, showing the elongation of the adhesive filaments. Urahama and co-authors [5, 6] revealed the importance of the stringiness in a peel test. Kano *et al.* [7] studied the peeling morphology of various acrylic adhesives and observed saw-tooth mechanisms from below (two-dimensional photographs). They explained these phenomena by the different dynamic shear properties as well as their mean relaxation times using a fluorescence depolarization technique. Benyahia *et al.* [8] did a systematic observation of the mechanisms of peeling as we move along the peeling master curve. They revealed that in most regimes studied, the elongational properties become predominant. This is very important, because the usual PSAs (Pressure Sensitive Adhesives) undergo strain hardening during elongation, as revealed by Verdier *et al.* [9], thus increasing the stresses by a factor of at least ten. This will also affect the peeling energy drastically.

Simple models have been constructed [10–13] which attempted to determine the peeling energy as a function of the velocity of peel. They usually assume that the peeling energy necessary to pull the strip (adhesive/backing) away from the substrate is mainly governed by the extension of the adhesive in the peeling region. Recently [9], the observation of regularly-spaced filaments and ribs has lead to the improvement of these models, in the case of the adhesion of a PSA on a Pyrex™ substrate. This model uses actual measurements of the dimensions of the ribs (filaments) to determine the extension of the adhesive element at the edge of the peeling front. This model was improved later [14] by considering a complete distribution of relaxation times to fit the rheometrical results, thus improving the prediction of the adhesion energy on Pyrex™.

It is now clear that a close observation of the mechanisms of flow is essential, if one wants to understand the complexity of peel adhesion.

To be able to go further and generalize these models, we pose the question of the universality of such observations, and of their application to other classes of adhesives. Do most adhesives show similar patterns? Can we extend the previous assumptions to any adhesive? Actually, one knows that changes in the shape of the peeling master curves already reveal probable changes in the mechanisms of flow.

This paper follows a previous one [8], and we propose to investigate another class of adhesives (acrylic-based adhesives) in order to determine simultaneously:

- peeling master curves $G = G(a_T V)$
  (G = energy restitution rate, a_T = temperature dependent coefficient, V = peeling speed)
- mechanisms of peeling observed with a fixed-point peeling machine
- rheometrical data (in shear and elongation)
- surface energies

This study will be conducted with two acrylic adhesives, with similar composition and surface properties, but different rheometrical properties: one is an uncross-linked adhesive, hence a viscoelastic liquid, and the other one is slightly cross-linked, *i.e.*, an elastico-viscous chemical gel. The reason for doing this, is that peeling curves of cross-linked adhesives (see Maugis *et al.*, for example [15]) generally show an interfacial branch, whereas peeling curves with uncross-linked adhesives [1, 3, 8] are usually divided into two parts: a cohesive failure mode, and an interfacial one. When peeling an elastomer, the cohesive branch may be absent, or displaced, due to the high forces necessary to elongate the adhesive mass, and to initiate a tearing mode of separation of the adhesive into two parts. Actually, these regimes are also governed by the surface properties of the adhesive and the substrate [14].

In the first part (Section 2), we describe the two adhesives. Rheometrical characterization in shear and elongation are detailed. Also, determination of the surface energy properties of both adhesives and the Pyrex^{TM} substrate are given.

In the next part (Section 3), we analyze the peeling master curves obtained for the two adhesives. Mechanisms of flows are carefully analyzed and compared with the ones from the previous study [8]. A generalization is proposed.

Finally, in the last part (Section 4), we discuss the application of previous theories [9] to the case of acrylic adhesives. Particular attention is focused on the effect of surface energies and the rheology of the adhesives.

2. MATERIALS AND RHEOMETRICAL PROPERTIES

Materials

The two adhesives (A and B) are statistical copolymers obtained by mixing of different acrylic comonomers. From a surface energy point of view, some of the elements are hydrophilic (Acrylic acid, Vinyl) and others are hydrophobic (2-Ethyl-Hexyl-Acrylate, Butyl Acrylate). In the end, the adhesive can develop good adhesion on polar and non-polar surfaces [16]. This is interesting in our case for the adhesives are intended to be used on skin ($T \approx 35°C$).

The two adhesives A and B have the same composition but the adhesive A is slightly cross-linked and the adhesive B is not.

The adhesives (100 μm thickness) are coated onto a Polyester backing (Hoechst RN 23, thickness 23 μm) in a solvent solution. Solvent is evaporated at 50°C for 30 min. The solvent is a complex mixture, and it was checked that less than 0.05% of it is left within the adhesive after evaporation. The adhesive is covered with a siliconed Polyester sheet (Hoechst), which will be removed just before application on the Pyrex™ substrate.

Pyrex™ is cleaned using a specific protocol already presented [8]: it starts with a pretreatment with acetone, followed by a bath in a sulfochromic-acid solution. Finally the substrate is cleaned with distilled water and dried in a vacuum oven at 50°C.

Rheometrical Measurements

a) Dynamic Shear Master Curves

Dynamic shear measurements were carried out on a Carrimed CS 100, using a cone and plate geometry (radius = 20 mm, angle = 4°) in the frequency range [10^{-2} Hz – 10 Hz], at temperatures ranging from

$-10°C$ to $50°C$. Figures 1 and 2 show master curves of moduli G' and G'' (respectively, storage and loss moduli) *versus* $a'_T\omega$ obtained using the time/temperature superposition principle [17, 18]. This principle works well in this case, although the adhesives are mixtures of different components. This is due to the fact that most components are of the same kind, and are compatible with each other. In addition, shift factors a'_T are compared with the ones obtained by shifting peeling curves (a_T). This is shown in Figure 3. We find good agreement between the coefficients obtained in rheometry and in the peeling experiments. Also, no significant difference is to be noted for the two adhesives A and B, because they have similar molecular structures.

The curves showing G' and G'' have a different behavior, especially at low values of the reduced frequency $a'_T\omega$. Adhesive A shows a plateau for G' and G'' at low frequencies, revealing the presence of an elastic network built through cross-links. It should still be present, had we gone to even lower frequencies. On the other hand, adhesive B does not show this behavior, and low values of the frequency correspond to

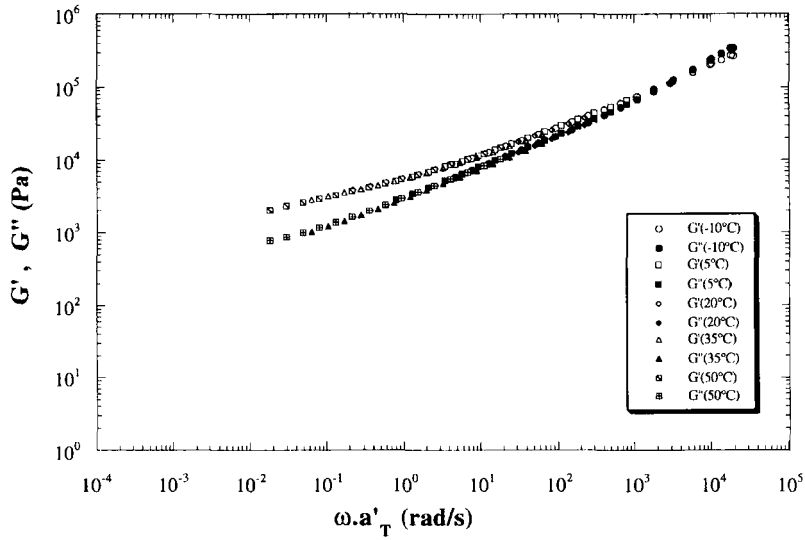

FIGURE 1 Master curve of shear moduli G' and G'': adhesive A ($T_{ref} = 35°C$).

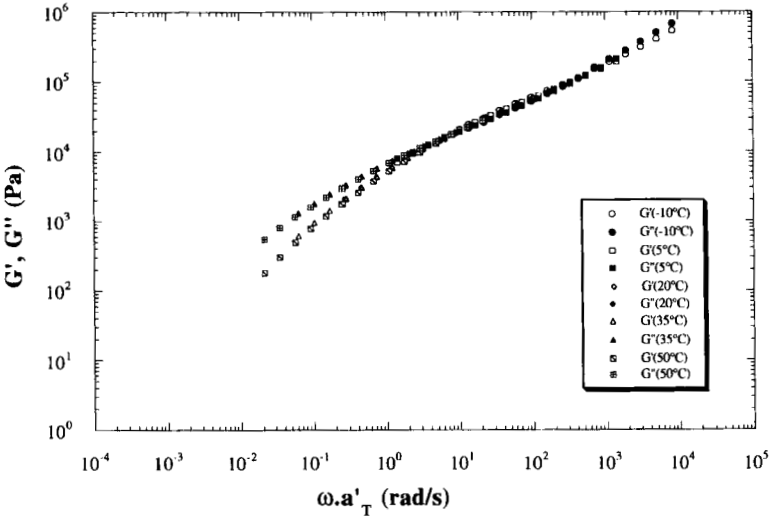

FIGURE 2 Master curve of shear moduli G' and G'': adhesive B (T_{ref} = 35°C).

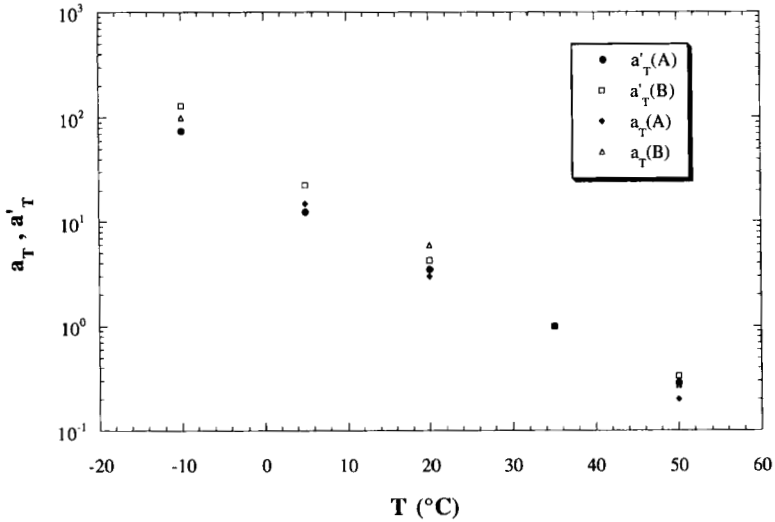

FIGURE 3 Comparison of a'_T and a_T for adhesives A and B.

typical slopes of 1 and 2, respectively, for G'' and G'. This is in agreement with the Newtonian behavior, and this is what we expect since B is an uncross-linked adhesive.

At high frequencies, moduli G' and G'' behave in the same way (both for A and B), with slopes of approximately 0.5. Such slopes are characteristic of gel systems, as found by Winter and Chambon [19]: chemical gels show congruence of moduli G' and G'' over a few decades in frequency with a G' modulus larger than G'' at lower frequencies, thus adhesive A is above the gel point, whereas B is not.

Finally, in the case of adhesive B, the plateau region is short, although the molecular weight is high (Mw = 270000, Ip $\approx$ 4). This is due to the fact that interactions between such molecules (hydrogen bonds) are strong and will prevent the mobility of chains, thus reducing the elasticity.

We will now study the elongational properties of adhesives A and B, which seem to be of real concern in adhesion related problems, as shown previously [9, 14].

b) Elongational Measurements

Elongational measurements have been carried out at ambient temperature ($T = 20°C$) using a two-roller machine, described previously by Gonzalez *et al.* [20]. Two rollers, 5 cm distant from each other, rotate in opposite directions at constant velocity, pulling on a material sample. This gives rise to a constant elongational rate, $\dot{\varepsilon}$, that we can change depending on the values of the velocity of rotation. Five different elongation rates have been used (0.029, 0.095, 0.38, 0.95, 1.9 s^{-1}).

The resulting rheometric function often used is the elongational viscosity $\eta^+(\dot{\varepsilon}, t)$ defined by Eq. (1)

$$\eta^+(\dot{\varepsilon}, t) = \frac{\sigma_{11} - \sigma_{22}}{\dot{\varepsilon}} \tag{1}$$

where $\sigma_{11} - \sigma_{22}$ represents the first normal stress difference (expressed in Pa).

The elongational viscosity typically shows a rapid increase (slope 1) corresponding to an elastic response, then it will either reach a plateau at low rates $\dot{\varepsilon}$ (η_E) or show a very rapid upturn corresponding to strain hardening, at higher rates.

Let us consider the two adhesives A and B. Figures 4 and 5 show the transient elongational viscosity as a function of time, and we observe

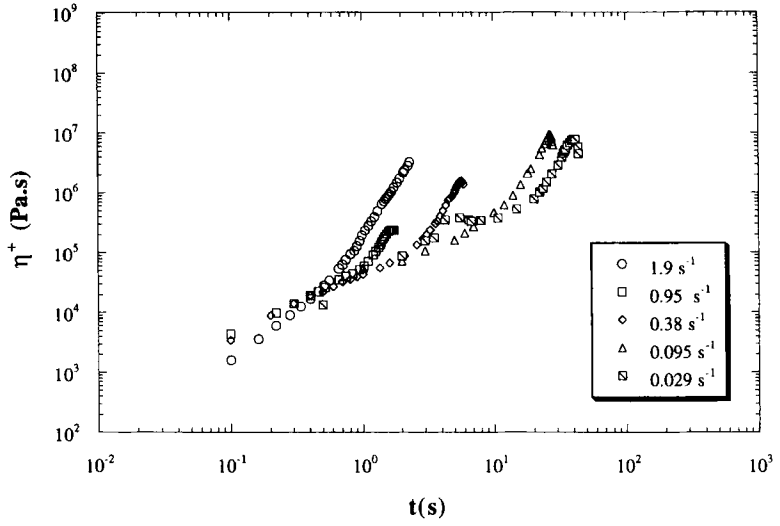

FIGURE 4 Elongational viscosity (adhesive A) at different elongational rates (T = 20°C).

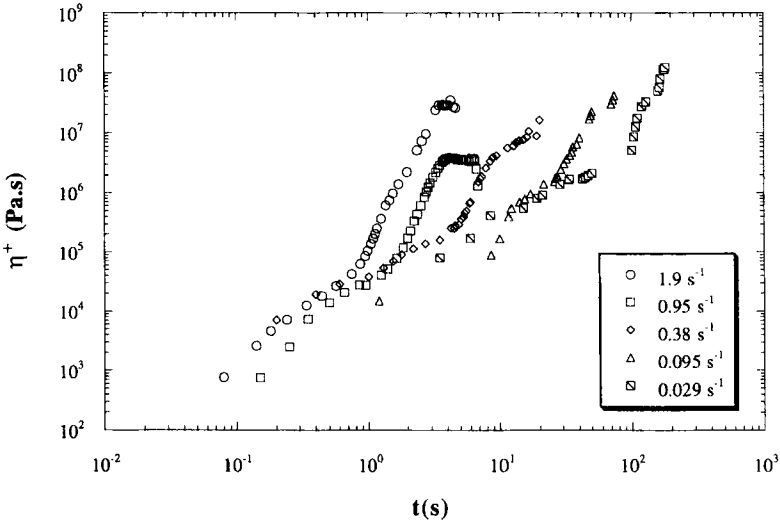

FIGURE 5 Elongational viscosity (adhesive B) at different elongational rates (T = 20°C).

strain hardening for both adhesives. The upturn seems to appear at smaller times for adhesive A, compared with the uncross-linked adhesive B. This makes sense, because the cross-linked adhesive A should show a rubbery behavior sooner compared with B, because of its structure (presence of cross-links). Also, when strain hardening occurs, the adhesive A breaks sooner, in an irreversible manner, whereas adhesive B resists up to longer times.

Surface Energy Measurements

As done previously [8], we determine the surface energy properties of the adhesives, the substrate (Pyrex™), and the backing (Polyester). We have used the classical decomposition $\gamma = \gamma^d + \gamma^p$ (γ, γ^d, γ^p, are the respective surface free energy, its dispersive component, its polar component). In addition, the adhesion energy, w, between a solid (surface free energy γ_s) and a liquid (surface tension γ_l) has been given by Fowkes [21], and further extended by Owens and Wendt [22], as in Eq. (2):

$$w = \gamma_l(1 + \cos\theta) = \gamma_s + \gamma_l - \gamma_{sl} \approx 2\sqrt{\gamma_s{}^d\gamma_l{}^d} + 2\sqrt{\gamma_s{}^p\gamma_l{}^p} \qquad (2)$$

where θ is the angle measured with a goniometer (Face, CA-A) and γ_{sl} is the interfacial free energy between the given solid and a liquid.

The polar and dispersive components of the free surface energy of the different solids can be deduced from wetting measurements with known liquids [18]. The results for adhesives A and B as well as Pyrex™ and the Polyester backing are given in Table I. Errors (hysteresis, surface roughness) are also reported here.

The adhesives A and B have the same dispersive and polar components, thus cross-linking does not change the surface properties.

TABLE I Components of the free surface energy

	γ_s^d (mJ/m^2)	γ_s^p (mJ/m^2)	γ_s (mJ/m^2)
Pyrex™	34.6 ± 1.1	30.2 ± 2.0	64.8 ± 3.1
Polyester	42 ± 1.6	2.3 ± 1.2	43.3 ± 2.8
Adhesive A	13 ± 0.5	0.9 ± 0.5	13.9 ± 1.0
Adhesive B	13 ± 0.5	0.9 ± 0.5	13.9 ± 1.0

We note the presence of a small polar component γ_s^p, due to the presence of the unit — C=O which creates hydrogen bonds.

The reversible work of adhesion, w, of the different adhesives on both the substrate (s) and the backing (b) are given by $w_s = \gamma_a + \gamma_s - \gamma_{as}$ (respectively, $w_b = \gamma_a + \gamma_b - \gamma_{ab}$) with the same approximation, Eq. (2), and the spreading coefficients S_s or S_b are: $S_s = w_s - 2\gamma_a$ (respectively, $S_b = w_b - 2\gamma_a$), where γ_a is the adhesive free energy. Table II shows these numbers with the corresponding errors.

Again w and S are about the same for both adhesives, but this was expected from surface energy components. The value of w may be considered to be of the order of typical energies found on such substrates, but the high positive values of the spreading coefficients, S, have to be discussed here. Clearly, we may expect strong affinities between acrylic adhesives and the surfaces produced here, thus leading to large peeling energies. This fact is also emphasized by the work of Benyahia [18], where it is shown that a positive coefficient S can lead to very large peeling energies.

Finally, the close values of w for Pyrex™ and Polyester suggest that the adhesive may undergo cohesive failure at some point, due to equal strengths on both sides, as is suggested by Benyahia *et al.* [8] when noticing the appearance of a fourth cohesive regime of peeling (on a substrate of PMMA) at even high values of the velocity.

3. PEELING MASTER CURVES AND ASSOCIATED MECHANISMS

Our attention now turns to peeling properties of the two different adhesives. The 90° peeling machine we used has been extensively

TABLE II Reversible work of adhesion, w, and spreading coefficient, S (mJm^{-2})

	Adhesive A	*Adhesive B*
Pyrex™ (w_s)	52.8 ± 5.2	52.8 ± 5.2
Polyester (w_b)	49.6 ± 3.3	49.6 ± 3.3
Pyrex™ (S_s)	25.0 ± 3.6	25.0 ± 3.6
Polyester (S_b)	21.8 ± 2.4	21.8 ± 2.4

described elsewhere [8, 9, 18]. It enables us to carry out experiments at constant peeling velocity (V), with a fixed peeling front. Therefore, we can film the peeling front and exhibit photographs of the different flow regimes. Temperature is controlled [$-10°C$, $50°C$], as well as relative humidity. We determine the force, $F(N)$, required to separate the adhesive from the substrate (or the backing), and we plot $G\ (= F/\ell, \ell$ is the width of the adhesive strip), the energy restitution rate as a function of the reduced velocity $a_T V$. a_T is a shift factor depending on the temperature, which determines by what amount the plots of log G need to be translated along the log horizontal axis in order to superpose them onto the plot at the reference temperature. Values of a_T have been given in the previous section (Fig. 3).

Let us start first with the peeling properties of the slightly cross-linked adhesive A.

Peeling of Adhesive A on Pyrex™. Mechanisms

Figure 6 shows the peeling master curve of adhesive A on Pyrex™. Measurements have been carried out at $-10°C$, $-5°C$, $0°C$, $5°C$, $20°C$, $35°C$, and $50°C$. Humidity is maintained at its minimum, around 10%.

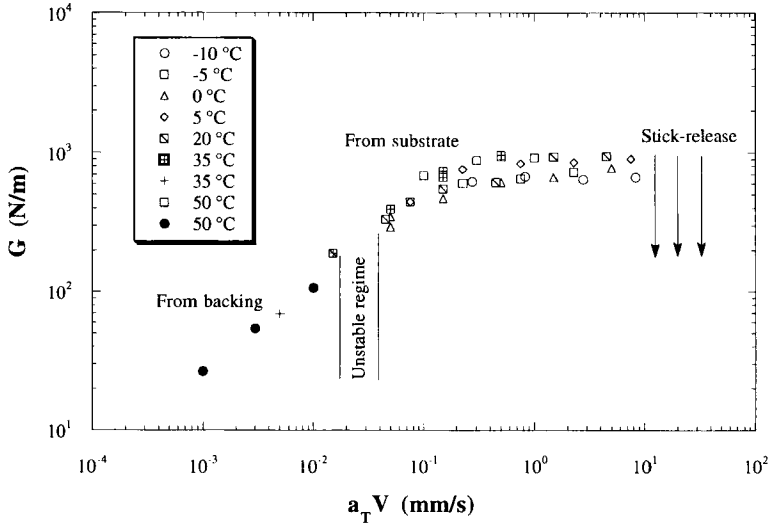

FIGURE 6 Peeling master curve of adhesive A on Pyrex™ substrate ($T_{ref} = 35°C$).

We will now describe the total peeling curve obtained as we increase the velocity, as well as the observed mechanisms (Fig. 7).

At slow peeling velocities, we observe interfacial failure at the *backing-adhesive interface*. We can associate a slope of about 0.7 (in logarithmic scale) to this part of the curve. Photographs 1 and 2 show the three-dimensional picture of the flow field. We will call this *mechanism* I'_1. We can clearly observe a fork formed at the edge at the adhesive/backing interface, which has been fed by the adhesive material present in the filaments. As we increase the velocity, the fork opens and one end will eventually meet the next fork's end. This mechanism is specific to cross-linked adhesives, because it was not observed in our previous study [8] with an uncross-linked adhesive. The study of adhesive B will also confirm this.

For a certain range of velocities ($a_T V \approx 0.02$ mm/s), we find next an *unstable zone*, where the solution tries to bifurcate to another regime without any success. Random force signals are reported. This may be due to the fact that the Dupré adhesion energies for adhesive A on Pyrex™ and Polyester are very close, so that the flow field is very

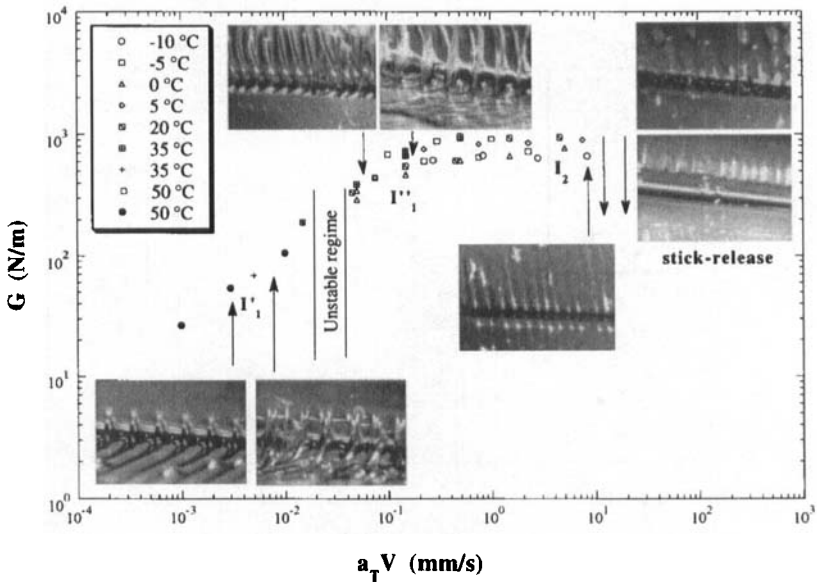

FIGURE 7 Peeling mechanisms of adhesive A on Pyrex™ substrate (T_{ref} = 35°C).

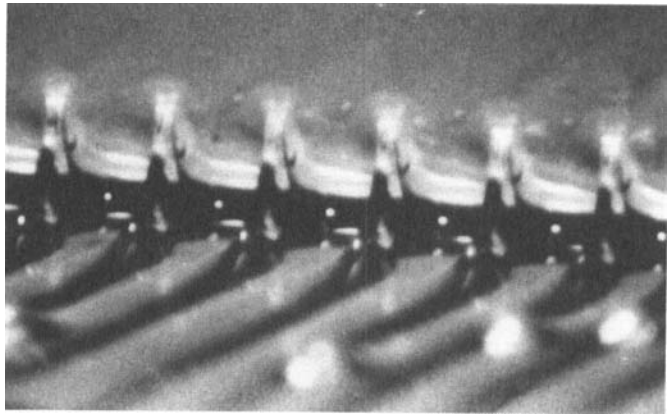

PHOTO 1 Mechanism I'_1: $T = 50°C$, $V = 0.015$ mm/s.

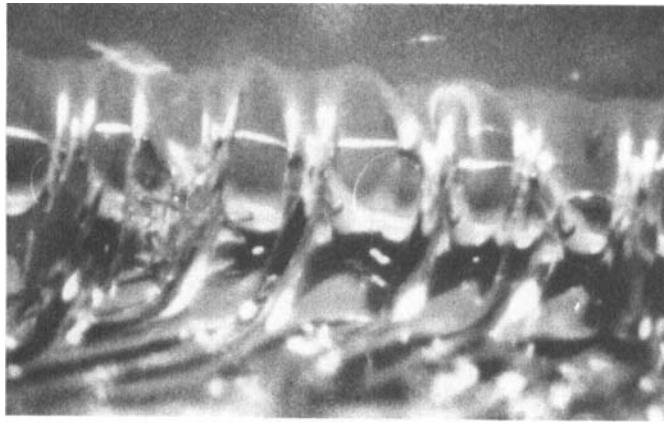

PHOTO 2 Mechanism I'_1: $T = 50°C$, $V = 0.15$ mm/s.

sensitive to the boundary conditions. The regime is actually undergoing a transition from interfacial failure at the backing to interfacial failure at the substrate. It is deduced that there are two branches, corresponding to peeling from the substrate and peeling from the backing:

- at low velocities, peeling from the backing is the stable one.
- at high velocities, peeling from the substrate is the stable branch.

The transition from one branch to the other is due to a change in the local condition of detachment. This will be explained in the last part. The key point is to introduce a new local failure criterion, including both surface energies and rheology, showing these combined effects. This idea may also be used for investigating regime changes in other systems.

At a reduced velocity of about 0.05 mm/s, we obtain a new steady regime of force, but this time it is associated with interfacial failure at the *adhesive/substrate interface*. It exhibits a new *mechanism* I_1'', which may be described as follows: it resembles the previously observed I_1', with the appearance of a fork with two ends which move towards each other, as we increase $a_T V$ (see Photograph 3). As the velocity gets higher, the fork edges meet, and air is trapped inside two thin sails of adhesive (Photograph 4). The pattern resembles a honeycomb structure. Compared with the previous case (slow velocities), the roles of the backing and substrate are inverted. This final mechanism was observed by Urahama [5] in the peeling of a weakly cross-linked adhesive, although (on his drawings) the sails are not clearly seen. Still, this emphasizes the fact that such a mechanism is only present with cross-linked adhesives.

As we move along the master curve, we next see a different flow field, corresponding to Photograph 5, and *mechanism* I_2. Three-dimensional flow is observed, with regular filaments forming goose-

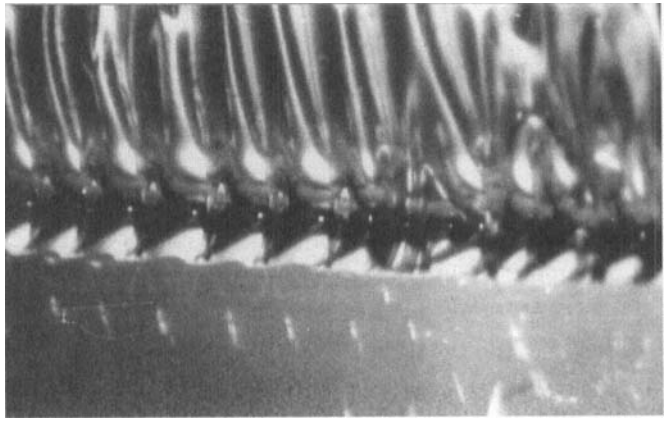

PHOTO 3 Mechanism I_1'': $T = 20°C$, $V = 0.005$ mm/s.

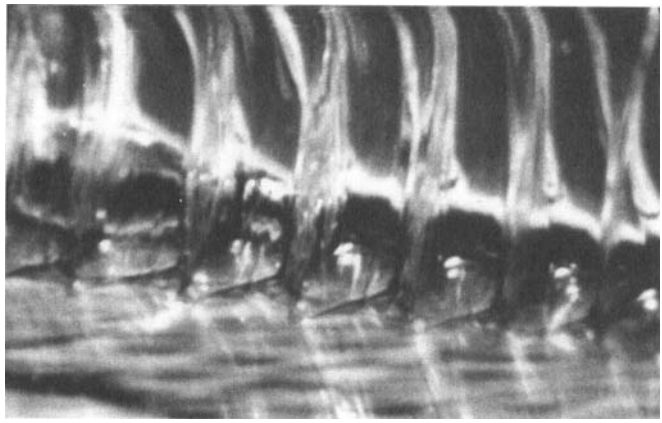

PHOTO 4 Mechanism I_1'': $T = 5°C$, $V = 0.005$ mm/s.

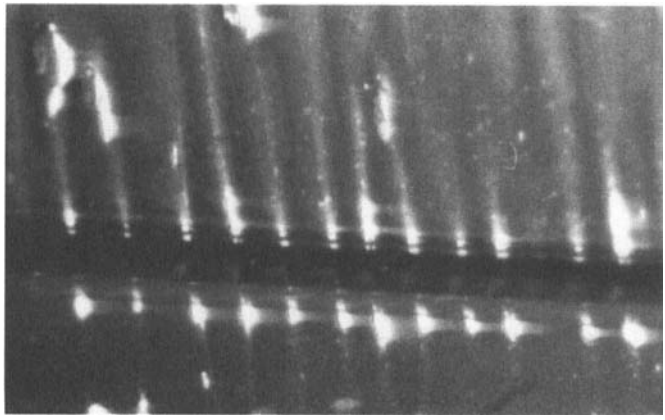

PHOTO 5 Mechanism I_2: $T = -10°C$, $V = 0.15$ mm/s.

like feet. This mechanism has already been observed by the authors [8], with an uncross-linked adhesive, and appears to be common to cross-linked and uncross-linked adhesives. At this stage, the peeling energy has stopped increasing and reaches a plateau. This behavior is similar to that observed by Barquins and Pouchelon [23] when looking at the adherence of silicone on stainless steel.

Finally, at high reduced velocities larger than 10 mm/s, we observe an *unstable regime of force* which is similar to the one described by

Benyahia *et al.* [8], called *stick-release*. The adhesive is first put in tension through its backing, without being peeled (Photograph 6), then it cannot withhold the tension, and allows the propagation of a crack (velocity $V_c > V$) at the interface. The adhesive is then released (Photograph 7). This is accompanied by a periodic regime of force.

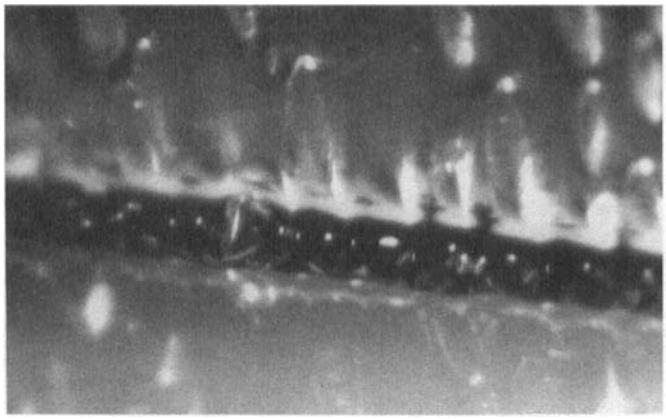

PHOTO 6 Stick-release, before detachment: $T = 0°C$, $V = 1.5$ mm/s.

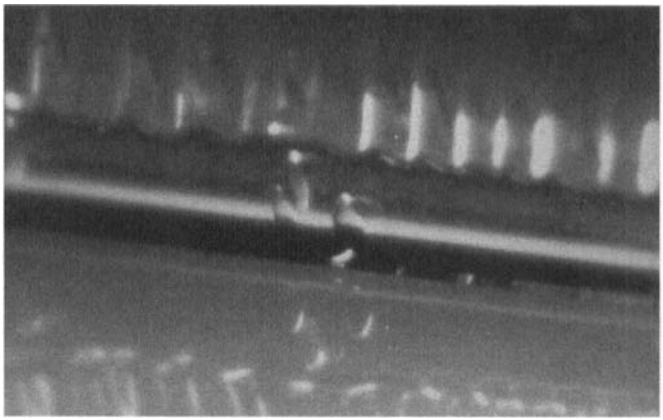

PHOTO 7 Stick-release, after detachment: $T = 0°C$, $V = 1.5$ mm/s.

Peeling of Adhesive B on Pyrex™

Figure 8 presents the peeling master curve of the adhesive B on the Pyrex™ substrate at $T_{ref} = 35°C$. Temperatures $-10°C$, 20°C, 35°C, 50°C have been used to achieve superposition.

In the stable regime, the failure observed is *cohesive* over the entire range of reduced velocities used. We can distinguish a linear part (slope 1 in logarithmic scale) which ends with a plateau at the higher peeling velocities. In comparison with the peeling curve of the slightly cross-linked adhesive A (Fig. 6), we can see that the effect of cross-linking has increased the peeling energies and has created changes in the slopes. However, the two curves show the same behavior at higher peeling velocities ($G \approx 1000$ N/m).

The mechanisms of flow observed in the case of the uncross-linked adhesive B have been observed before [8], so we will not go into details here: there is only one mechanism here which is similar to mechanism C_2 in [7]. It is a three-dimensional one, characterized by the formation of long regular ribs, such as the ones observed in hydrodynamic instabilities (see for example Coyle *et al.* [24]) occurring at a free surface.

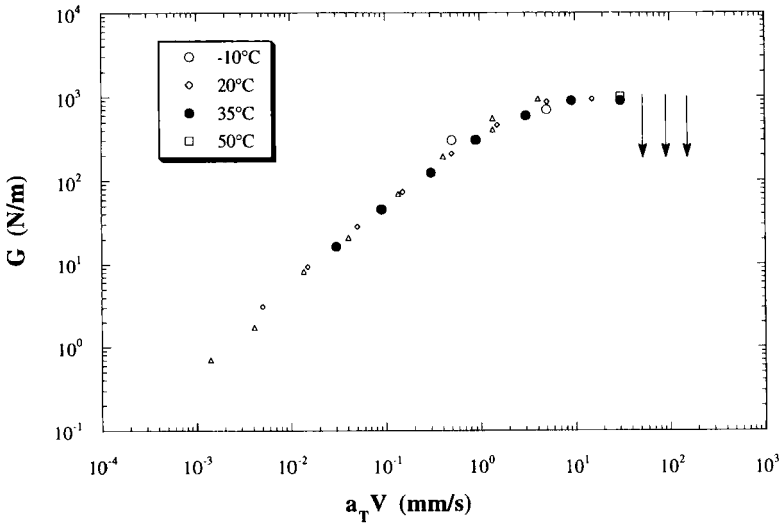

FIGURE 8 Peeling master curve of adhesive B on Pyrex™ substrate ($T_{ref} = 35°C$).

At high velocities, an unstable regime occurs, which may correspond to the beginning of the transition from cohesive to interfacial failure. We could not go to higher velocities so no interfacial failure is reported.

4. DISCUSSION

Mechanisms of Failure

We will first review and classify the different mechanisms of peeling obtained on cross-linked and uncross-linked adhesives. In our first paper [8], we determined four mechanisms of flow in cohesive failure for an uncross-linked adhesive. They are referred to as C_1, C_2, C_3, C_4 (note that C_4 was only obtained on a Plexiglas^{TM} substrate). For the interfacial type of failure, we found two different stable regimes I_1, I_2, and the unstable stick-release mechanism. Mechanism C_2 has also been observed with the uncross-linked acrylic adhesive B. Thus, we can generalize our first results [8] and assume them to be present for all uncross-linked adhesives.

In the case of the cross-linked adhesive, we only obtained interfacial failure, associated with mechanisms I_1', I_1'' and I_2. Still, it may be possible to obtain cohesive failure, but in the case of a higher surface energy substrate. This will be discussed in the next part.

To summarize this, Table III gives the mechanisms that were observed on our adhesives:

TABLE III Mechanisms of peeling

Uncross-linked adhesive	*Cross-linked adhesive*
cohesive: C_1, C_2, C_3 and C_4	cohesive: not observed
interfacial: I_1 and I_2	interfacial: I_1', I_1'' and I_2
stick-release	stick-release

Influence of the Degree of Cross-linking

From our results, we were not able to obtain cohesive failure with the slightly cross-linked adhesive A. Furthermore, cohesive failure has not been reported for such adhesives by Barquins and co-authors [15, 23],

but their studies are carried out using rubbers or highly cross-linked materials on low energy surfaces. Dahler and Pouchelon [25] have shown that it is possible to obtain cohesive failure with slightly cross-linked adhesives (*e.g.*, silicones cross-linked with peroxide), but they used a primer between the adhesive and the substrate. We may say that, depending on the level of cross-linking agent and specific surface preparations, cohesive failure can be obtained. Figure 9 summarizes these comments, when the percentage of cross-linking agent is varied, at fixed surface properties. The change in the curves, indicated by the arrow, corresponds to increasing degree of cross-linking. Two cases may occur:

a) When the substrate has a *low surface energy*, it is possible to obtain cohesive and interfacial failure. When adding small amounts of cross-linking agent, the cohesive branch starts with a higher value (Carré and Schultz [26]), but lower values of the peak are expected on the cohesive branch, because this peak is mainly related to the appearance of fibrillation. It is clear that a cross-linked adhesive will show less fibrillation. The interfacial branch will show higher energies (this study) as the degree of cross-linking increases; this will make the two branches close to each other until a critical value of the degree of cross-linking is reached, at which they will possibly merge.
b) On the other hand, a *high surface energy substrate* will prevent the appearance of an interfacial branch, because of the high energy

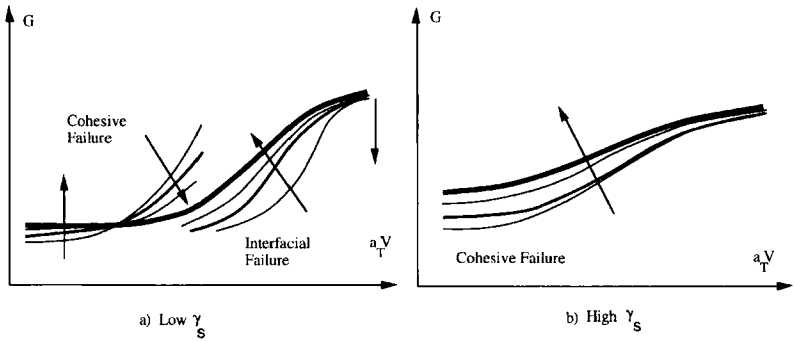

FIGURE 9 Peeling master curves for an adhesive with different increasing percentages of cross-linking agent (direction shown by arrow) a) Low surface energy substrate; b) High surface energy substrate.

between the substrate and the adhesive. Cohesive curves will be expected, and the values of G will increase with increasing degree of cross-linking. This should be due to higher cohesive strengthening of the adhesive.

Effects of Rheometric Properties

Next we consider the influence of rheometric and surface properties and their combined effects on peeling curves. The measured moduli G' and G'' have shown similar behaviors, except for small angular velocity, ω, where a plateau was obtained for adhesive A. These moduli can give an idea of the comparison between type of failure and type of mechanical behavior [8]. On the other hand, they do not give estimates of the orders of magnitude of the peeling energy, G. Actually G can be predicted [9, 14] using elongational experiments, when the adhesive is uncross-linked, and when regular filaments or ribs are observed. In the case of the cross-linked adhesive, things may become more complicated, because of the complexity of the flow pattern observed.

Anyway, the presence of elongational flows is also clear, as on Photographs 1–3, or when looking at the sails formed on Photograph 4. We will not try here to compare quantitatively the curves obtained. Nevertheless, let us consider the elongational properties of the adhesives A and B. From the constant rate experiments, it is shown that A will undergo strain hardening sooner (timewise) than B, as well as a sudden break-up; therefore, we expect stronger resistance of adhesive A. This is what can be deduced by comparison of Figures 6 and 8: stresses, therefore values of G, are higher by a decade when peeling adhesive A, even though we only obtain interfacial failure.

Combined Effects of Rheometric Properties and Surface Energies

In addition to the elongational properties, one needs to take into account surface energy data. For both adhesives, we have measured the same free surface energy, but the peeling results are quite different: interfacial failure is obtained with adhesive A whereas cohesive failure is obtained for adhesive B. Therefore, one needs to account for the effect of cross-linking. Let us recall a previous result by Carré and

Schultz [26]: they obtained parallel cohesive curves on aluminum for various adhesives and deduced a so-called w_c cohesive energy, larger than the classical term $2\gamma_a$. They suggest that the cohesive energy should be modified by adding a chemical contribution, W_{chem} (holding for entanglements in the network), to the cohesive energy, w_c. This will be particularly the case when dealing with cross-linked elastomers, where the cohesion energy is clearly higher. This contribution can reach values of up to $70\,\text{mJ/m}^2$ or more (in the case of NBR, W_{chem} can be evaluated to lie between 22 and $35\,\text{mJ/m}^2$ from [26]). This will change the value of w_c in the case of the cross-linked adhesive A, where cross-links exist. We assume that $2\gamma_a$ is increased (by say approximately $30\,\text{mJ/m}^2$), therefore S_s and S_b will become negative (definitions of all the parameters have been given in the section on Surface Energy Measurements).

This leads to the following conclusions, *at low velocities*, V.

a) $S_s > 0$ and $S_b > 0$ The Dupré adhesion energy is larger than the cohesive energy.
Failure will be in the bulk: *cohesive failure* → adhesive B

b) $S_s < 0$ or $S_b < 0$ *interfacial failure*
Comparison between w_b (backing) and w_s (substrate) is needed to determine on which side we will have interfacial failure

$w_s > w_b$ failure is at backing/adhesive interface → adhesive A (low V)

These results only work for small velocities, because the rheometric effects are negligible. If we *increase the velocity*, rheology comes into play, as proposed in [14]. We expect a bound for the velocity to change to interfacial failure at the substrate.

The dissipative effects at the corner (nip) or detachment point can be introduced in the case of interfacial failure. de Gennes [27] has proposed to rewrite Young's relation. We may write, assuming first that the viscosity is constant (and large), and that the angle θ is small:

$$\gamma_s - \gamma_{as} - \gamma_a \cos\theta = \frac{3\eta V}{\theta} \operatorname{Ln}\left(\frac{L\theta}{a}\right) \tag{3}$$

which may again be written in terms of the spreading coefficient, S:

$$S + \gamma_a (1 - \cos\theta) = \frac{3\eta V}{\theta} \operatorname{Ln}\left(\frac{L\theta}{a}\right) \tag{4}$$

where L is a macroscopic size (the adhesive thickness, for example) and a is a molecular length. Inspection of the graphs of the two functions (on the right and left hand side of Eq. (4)) for small values of the angle θ is shown in Figure 10. There is always a small angle, θ, which is a solution of Eq. (4) but only when V is large enough. The critical velocity, V^*, is a function of the parameters in Eq. (4). The condition can be written:

$$V > V^*(L, a, \eta, S, \gamma_a) \tag{5}$$

Also, we may note that if Eq. (5) is satisfied, two solutions, θ_1 and θ_2 are possible, one stable, and the other one unstable.

In any case, these expressions show the combined role of the surface and rheometric properties in determining the type of failure. Further-

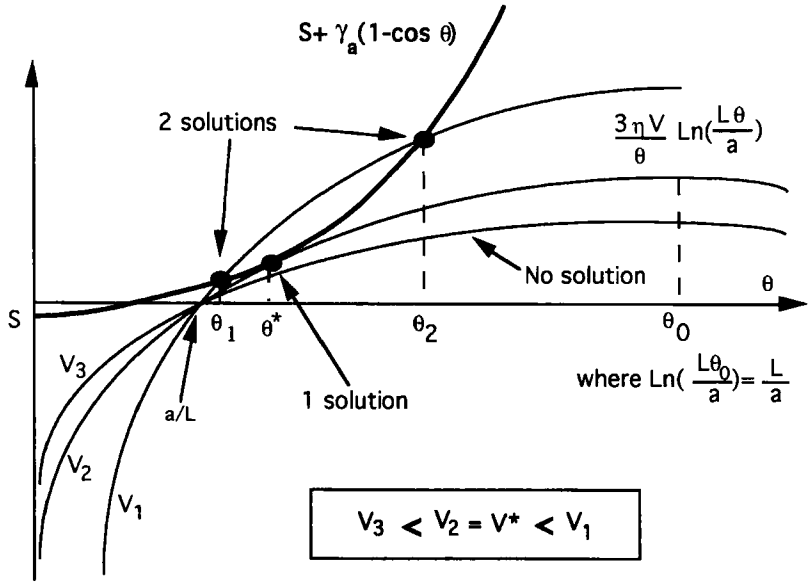

FIGURE 10 Condition on the velocity to obtain interfacial failure from substrate.

more, by making Eq. (3) into a dimensionless form, we obtain the relevant dimensionless groups: $(\gamma_a/\eta V)$, $(\gamma_s/\eta V)$, $(\gamma_{as}/\eta V)$, $(\gamma_b/\eta V)$, $(\gamma_{ab}/\eta V)$ and, of course, (T/T_{ref}) (T = temperature, T_{ref} = reference temperature).

There are no references in the literature for calculating the dissipation in the corner, in the case of a viscoelastic material. We may then replace the viscosity, η, by its equivalent when it exists. The viscosity is, in fact, shear rate dependent and its value is $\eta(\dot{\gamma})$, where $\dot{\gamma}$ is the shear rate and is velocity dependent. In the case considered, estimations of the viscosity lead to a dependence of ηV as a power law V^n, where $0 < n < 1$. This does not change the qualitative aspect of the curves in Figure 10.

For a more accurate description, the rheology will be introduced *via* a Weissenberg number, $(a_T V \lambda_1/e)$ (λ_1 = a relaxation time and e = thickness), which will play a role by modification of the viscosity. Other relaxation times will be added to describe the material's behavior completely.

Therefore, this simple analysis shows that a criterion of the type

$$f\left(\frac{\gamma_a}{\eta V}, \frac{\gamma_s}{\eta V}, \frac{\gamma_{as}}{\eta V}, \frac{\gamma_b}{\eta V}, \frac{\gamma_{ab}}{\eta V}, \frac{T}{T_{\text{ref}}}, \frac{a_T V \lambda_1}{e}\right) = 0 \qquad (6)$$

is needed to explain the transition from a cohesive to an interfacial regime. This idea is relevant to the study of adhesives A and B and may be used further in the study of other systems.

5. CONCLUSIONS

In this paper, we have discussed the type of peeling curves and mechanisms of peeling that can be obtained for a family of acrylic adhesives.

We have shown that classes of mechanisms are mainly determined by the amount of cross-links present in the adhesive.

The shapes of the peeling master curves also are functions of the degree of cross-linking, and the cohesive branch disappears eventually for a highly cross-linked adhesive.

The type of regime is governed by the combined effects of the rheology and the surface energies, in a complex manner.

Further studies are needed to quantify the critical velocity for which the system goes from cohesive to interfacial failure.

Acknowledgements

We would like to address special thanks to C. Mikler and D. Dhuique-Mayer (Laboratoires Fournier) for their constant help and sponsorship throughout this study.

References

[1] Kaelble, D. H., *J. Adhesion* **1**, 102 (1969).
[2] Kaelble, D. H., *Trans. Soc. Rheol.* **IV**, 45 (1960).
[3] Niesiolowski, F. and Aubrey, D. W., *J. Adhesion* **13**, 87 (1981).
[4] Zosel, A., *Double Liaison–Physique et chimie des peintures et adhésifs* **431/432**, 275 (1991).
[5] Urahama, Y., *J. Adhesion* **31**, 47 (1989).
[6] Miyagi, Z., Koike, M., Urahama, Y. and Yamamoto, K., *Int. J. Adhesion Adhesives* **14**(1), 39 (1994).
[7] Kano, Y., Ushiki, H. and Akiyama, S., *J. Adhesion* **43**, 223 (1993).
[8] Benyahia, L., Verdier, C. and Piau, J.-M., *J. Adhesion* **62**, 45 (1997).
[9] Verdier, C., Piau, J.-M. and Benyahia, L., *C. R. Acad. Sci. Paris Série IIb* **t.323**, 739 (1996).
[10] Gent, A. N. and Petrich, R. P., *Proc. Roy. Soc.* **A310**, 433 (1969).
[11] Connelly, R. W., Parsons, W. F. and Pearson, G. H., *J. Rheol.* **25**(3), 315 (1981).
[12] Gupta, R. K., *J. Rheol.* **27**(2), 171 (1983).
[13] Good, R. J. and Gupta, R. K., *J. Adhesion* **26**, 13 (1988).
[14] Piau, J.-M., Verdier, C. and Benyahia, L., *Rheol. Acta.* **36**, 449 (1997).
[15] Maugis, D. and Barquins, M., *J. Phys. D: Appl. Phys.* **11**, 1989 (1978).
[16] Kenney, J. F., Haddock, T. H., Sun, R. L. and Parreira, H. C., *J. Appl. Polym. Sci.* **45**(2), 355 (1992).
[17] Williams, M. L., Landel, R. F. and Ferry, J. D., *J. Amer. Chem. Soc.* **77**, 3701 (1955).
[18] Benyahia, L., Relations entre les propriétés rhéologiques et physico-chimiques des polymères et leurs propriétés adhésives. Application à la Peau. *PhD Thesis*, Université de Grenoble, 1996.
[19] Winter, H. H. and Chambon, F., *J. Rheol.* **30**(2), 367 (1986).
[20] Gonzalez-Alvarez, A., d'Assenza, G., Legrand, J.-F. and Piau, J.-M., *C. R. Acad. Sci. Paris Série II* **t.320**, 23 (1995).
[21] Fowkes, F. M., *J. Phys. Chem.* **67**, 2538 (1963).
[22] Owens, D. K. and Wendt, R. C., *J. Appl. Polym. Sci.* **13**, 1741 (1969).
[23] Barquins, M. and Pouchelon, A., *Caoutchoucs et Plastiques* **676**, 105 (1988).
[24] Coyle, D. J., Macosko, C. W. and Scriven, L. E., *J. Fluid Mech.* **171**, 181 (1986).
[25] Dhaler, D. and Pouchelon, A., Euradh. 92, Karlsruhe, 1992.
[26] Carré, A. and Schultz, J., *J. Adhesion* **17**, 135 (1984).
[27] de Gennes, P.-G., *Reviews of Modern Physics* **57**(3), Part 1, 827 (1985).